Title

CIITA induces expression of MHC-I and MHC-II in transmissible cancers

Running title

Regulation of MHC by CIITA in DFT cells

Authors

Chrissie E. B. Ong[1], Yuanyuan Cheng[2], Hannah V. Siddle[3,4], A. Bruce Lyons[5], Gregory M. Woods[1], Andrew S. Flies[1*]

Affiliations

[1]Menzies Institute for Medical Research, College of Health and Medicine, University of Tasmania, Hobart, TAS, Australia

[2]School of Life and Environmental Sciences, The University of Sydney, Sydney, NSW, Australia

[3]Department of Biological Sciences, University of Southampton, Southampton, UK

[4]Institute for Life Sciences, University of Southampton, Southampton, UK

[5]Tasmanian School of Medicine, College of Health and Medicine, University of Tasmania, Hobart, TAS, Australia

*Correspondence

Andrew S. Flies, PhD

Menzies Institute for Medical Research, College of Health and Medicine

University of Tasmania

Private Bag 23, Hobart TAS 7000

phone: +61 3 6226 4614; email: Andy.Flies@utas.edu.au

Abstract

MHC-I and MHC-II molecules are critical components of antigen presentation and T cell immunity to pathogens and cancer. The two monoclonal transmissible devil facial tumours (DFT1, DFT2) exploit MHC-I pathways to overcome immunological anti-tumour and allogeneic barriers. This exploitation underpins the ongoing transmission of DFT cells across the wild Tasmanian devil population. We have previously shown that constitutive expression of NLRC5 can induce stable upregulation of MHC-I on DFT1 and DFT2 cells, but unlike IFNG-treated cells, NLRC5 does not upregulate PDL1. MHC-II expression is crucial for $CD4^+$ T cell activation and is primarily confined to haematopoietic antigen presenting cells. Transcriptomic analysis of DFT1 and DFT2 cell lines showed that several genes of the MHC-

I and MHC-II pathways were upregulated in response to constitutive overexpression of the class II transactivator (CIITA) gene. This was further supported by upregulation of MHC-I protein on DFT1 and DFT2 cells, but interestingly MHC-II protein was upregulated only on DFT1 cells. The functional significance of the MHC upregulation on DFT cells was shown using serum from devils with natural or immunotherapy-induced DFT1 regressions; binding of serum IgG was stronger in CIITA-transfected cells than wild type cells, but was less than binding to NLRC5 transfected cells. This new insight into regulation of MHC-I and MHC-II in cells that naturally overcome allogeneic barriers can inform vaccine, immunotherapy, and tissue transplant strategies for human and veterinary medicine.

Keywords

transmissible cancer, devil facial tumour, DFTD, allograft, MHC, CIITA

1. Introduction

The Tasmanian devil is the largest extant carnivorous marsupial and is endemic to the island state of Tasmania. Following the emergence of devil facial tumour disease (DFTD) in 1996, the population of devils has declined precipitously, threatening the persistence of devils in the wild[1]. DFTD is caused by two independent transmissible cancers of Schwann cell origin, referred herein as DFT1 and DFT2[2,3]. DFT1 was discovered northeast of Tasmania in 1996 while the second tumour, DFT2, was found in 2014 in the D'Entrecasteaux channel, southeast Tasmania. Both tumour types are clonal cell lines that harbour distinct genetic profiles differing from individual host devils[2,3]. DFT cells are transmitted as a malignant allograft amongst devils through social interactions.

Genetic differences between host and tumour, particularly at the major histocompatibility complex (MHC) loci[4], should induce immune-mediated allograft rejection. However, the 25 years of ongoing DFT1 transmission suggests that DFT1 cells have evolved to evade immune defences. The lack of anti-DFT immune responses has predominantly focused on the loss of MHC-I from the surface of DFT1 cells. This occurs via epigenetic downregulation of several components of the MHC-I antigen processing pathway[5] and a hemizygous deletion of beta-2 microglobulin (*B2M*), which is necessary for stabilising MHC-I complexes on the cell surface[6]. Natural and immunotherapy-induced tumour regressions have been observed in devils, along with antibody responses to DFT1 cells, albeit primarily in the context of MHC-I[7–9]. Conversely, the emerging DFT2 tumours do express MHC-I[10], suggesting that other immune evasion mechanisms are important.

Given the role of MHC-I in antigen display and anti-DFT humoral response, the manipulation of MHC-I expression on DFT cells is an attractive target to improve host responses towards DFT cells and mitigate the effects of disease in the wild devil population. An upregulation of MHC-I on DFT cells should enhance MHC-I-restricted tumour-specific cytotoxic $CD8^+$ T cell response. However, this approach alone proved to be insufficient for eliciting protective immunity, as exemplified in immunisation trials of naïve devils against DFT1[9]. Although $CD8^+$ T cells are recognised as the major effector cells in tumour elimination, $CD4^+$ T cell help is critical in facilitating an effective anti-tumour immune response. $CD4^+$ helper T cells play a multifaceted role of orchestrating the adaptive and humoral immune response. From cytokine production to expression of co-stimulatory molecules, $CD4^+$ helper T cells initiate, augment, and sustain the effector function of not only $CD8^+$ T cells and B cells but also innate cells[11–14]. Moreover, $CD4^+$ T cells are capable of initiating allograft rejection independently of $CD8^+$ T cells[15,16].

The activation of $CD4^+$ T cells involves recognition of antigens presented on MHC-II complexes. In contrast to MHC-I, constitutive expression of MHC-II is restricted to thymic epithelial cells, activated human T cells, and professional antigen presenting cells (APCs) such as B cells, dendritic cells, and macrophages. However, *de novo* MHC-II expression can be induced in non-haematopoietic cells including tumour cells by the inflammatory cytokine interferon gamma (IFNG)[17]. Both constitutive and IFNG-induced expression of MHC-II genes are mediated by the Class II transactivator (CIITA), making it the master regulator of MHC-II expression[18,19]. Additionally, CIITA is capable of modulating the expression of MHC-I, particularly in cell lines with low to no MHC-I expression[20,21].

The presence of MHC-II molecules in DFT cells has not been described, although CIITA and some MHC-II transcripts can be upregulated *in vitro* in DFT1 cells with IFNG treatment[5]. We have previously genetically modified DFT1 and DFT2 cells that overexpress the MHC-I transactivator NLRC5 to induce stable expression of MHC-I on the cell surface[8]. The lack of MHC-II expression in DFT cells provided an opportunity to conduct similar investigations into the role of CIITA in MHC-II regulation in marsupials and transmissible cancers. Transcriptomic and protein-based analyses showed that CIITA upregulates the expression of genes associated with MHC-I and MHC-II antigen processing and presentation in DFT cells. The ability to modulate antigen presentation in transmissible cancer cells in the context of MHC uncovers additional targets for anti-tumour immune response and the potential for recruitment of $CD4^+$ T cell help.

2. Materials and methods

2.1 Cells and cell culture conditions

Cell lines that were used in this study include DFT1 cell line C5065 strain 3[22] (RRID:CVCL_LB79), and DFT2 cell lines: RV (RRID:CVCL_LB80) and JV (RRID:CVCL_A1TN)[3] (**Table 1**). DFT1 C5065 was provided by A-M Pearse and K. Swift of the Department of Primary Industries, Parks, Water and Environment (DPIPWE) (Hobart, TAS, Australia) and was previously established from DFT1 biopsies obtained under the approval of the Animal Ethics Committee of the Tasmanian Parks and Wildlife Service (permit numbers A0017090 and A0017550)[22]. DFT2 cell lines RV and JV were established from single cell suspensions obtained from tumour biopsies[3]. Cells were cultured at 35 °C with 5% CO_2 in Gibco™ RPMI 1640 medium with L-glutamine (Thermo Fisher Scientific, Waltham, MA, USA) supplemented with 10% heat-inactivated fetal bovine serum (Bovogen Biologicals, Melbourne, VIC, Australia), 1% (v/v) Gibco™ Antibiotic-Antimycotic (100X) (Thermo Fisher Scientific), 10 mM Gibco™ HEPES (Thermo Fisher Scientific) and 50 μM 2-mercaptoethanol (Sigma-Aldrich, St. Louis, MO, USA) (complete RPMI medium).

2.2 Plasmid construction

The coding sequence for full length devil *CIITA* (XM_023497584.2) was isolated from cDNA of devil peripheral blood mononuclear cells (PBMCs) by PCR using Q5® Hotstart High-Fidelity 2X Master Mix (New England Biolabs (NEB), Ipswich, MA, USA) (see **Supplementary Table 1** for list of primers and reaction conditions). Sleeping Beauty (SB) transposon plasmid pSBbi-BH[23] (a gift from Eric Kowarz; Addgene # 60515, Cambridge, MA, USA) was digested at SfiI sites (NEB) with the addition of Antarctic Phosphatase (NEB) to prevent re-ligation. Devil *CIITA* was then cloned into SfiI-digested pSBbi-BH using NEBuilder® HiFi DNA Assembly Cloning Kit (NEB). The assembled plasmid pCO2 was transformed into NEB® 5-alpha competent *Escherichia coli* (High Efficiency) (NEB) according to manufacturer's instructions (see **Supplementary Figure 1** for plasmid maps). Positive clones were identified by colony PCR and the plasmids were isolated using NucleoSpin® Plasmid EasyPure kit (Macherey-Nagel, Düren, Germany). The DNA sequence of the cloned devil *CIITA* transcript was verified by Sanger sequencing using Big Dye™ Terminator v3.1 Cycle Sequencing Kit (Applied Biosystems (ABI), Foster City, CA, USA) and Agencourt® CleanSEQ® (Beckman Coulter, Brea, CA, USA) per manufacturer's instructions. The sequences were analyzed on 3500xL Genetic Analyzer (ABI) (see **Supplementary Table**

2 for list of sequencing primers). For detailed step-by-step protocols for plasmid design and construction, reagent recipes, and generation of stable cell lines, see Bio-protocol # e3696[24].

2.3 Transfection and generation of stable cell lines

DFT1 and DFT2 cell line C5065 and JV, respectively, were transfected with plasmid pCO2 to generate stable cell lines that overexpress CIITA. DNA transfections were performed using polyethylenimine (PEI) (1 mg/mL, linear, 25 kDa; Polysciences, Warrington, FL, USA) at a 3:1 ratio of PEI to DNA (w/w) as previously described[8]. Briefly, DFT cells were co-transfected with pCO2 and SB transposase vector pCMV(CAT)T7-SB100[25] (a gift from Zsuzsanna Izsvak; Addgene plasmid # 34879) at a ratio of 3:1 in µg, respectively. One µg of total plasmid DNA was used per mL of culture volume. The cells were incubated with the transfection solution overnight at 35 °C with 5% CO_2. The media was removed and replaced with fresh complete RPMI medium. 48 h post-transfection, the cells were observed for expression of reporter gene mTagBFP. Positively-transfected cells were selected with 1 mg/mL hygromycin B (Sigma-Aldrich) for seven days before being maintained in 200 µg/mL hygromycin B in complete RPMI medium. The two tumour cell lines were also transfected with empty vector pSBbi-BH as controls.

2.4 RNA sequencing and analysis

RNA libraries were prepared, sequenced and processed as previously described[8,26,27]. **Table 1** shows the source of RNA samples used in this study. Briefly, RNA extraction (two replicates per cell line) was performed using the Nucleospin® RNA Plus Kit (Macherey-Nagel) following the manufacturer's instructions. mRNA libraries were prepared and sequenced at the Ramaciotti Centre for Genomics (Sydney, NSW, Australia). All RNA samples had RNA Integrity Number (RIN) scores of 10.0. Libraries were prepared using TruSeq Stranded mRNA Library Prep (Illumina Inc., San Diego, CA, USA) and single-end, 100-base pair sequencing were performed on an Illumina NovaSeq 6000 platform (Illumina). The quality of the sequencing reads was assessed using FastQC version 0.11.9[28]. Raw FASTQ files for DFT1.CIITA and DFT2.CIITA have been deposited to the European Nucleotide Archive (ENA) and are available at BioProject # PRJEB45867.

Subread version 2.0.0[29] was used to align sequencing reads to the Tasmanian devil reference genome (GCA_902635505.1 mSarHar1.11) and the number of reads mapped to a gene was counted using featureCounts[30]. The analysis of differentially expressed genes was performed using the statistical software R studio[31] on R version 4.0.0[32]. Genes with less than 100 aligned

reads across all samples were excluded from the analysis and raw library sizes were scaled using *calcNormFactors* in edgeR[33–35]. To account for varying sequencing depths between lanes, read counts were normalised by upper quartile normalisation using *betweenLaneNormalization* in EDASeq[36,37]. Gene length-related biases were normalised by scaling read counts to transcripts per kilobase million (TPM). Differential expression analysis was carried out using the *voom*[38] function in *limma*[39] with linear modelling and empirical Bayes moderation[40]. To isolate differentially expressed genes, gene expression of CIITA- or NLRC5-expressing cell lines (DFT.CIITA, DFT.NLRC5) was compared against vector-only control (DFT.BFP) while IFNG-treated cells (DFT.WT + IFNG) was compared against untreated cells (DFT.WT), according to their respective tumour origin. Genes were defined as significantly differentially expressed by applying false discovery rate (FDR) < 0.05, and $\log_2$ fold change (FC) ≥ 2.0 (upregulated) or ≤ −2.0 (downregulated) thresholds (see **Supplementary Table 3** for list of differentially expressed genes).

Venn diagrams of differentially expressed genes were developed using Venny version 2.1[41]. Heatmaps were created from $\log_2$(TPM) values using the ComplexHeatmap[42] package in R studio. For functional enrichment analysis, over-representation of gene ontology (GO) biological processes in the list of differentially expressed genes was performed using Database for Annotation, Visualization and Integrated Discovery (DAVID) functional annotation tool[43,44]. The Tasmanian devil *Sarcophilus harrisii* was applied as the species for gene lists and background. Significant GO terms (GOTERM_BP_ALL) were selected by applying the following thresholds: p-value < 0.05 and FDR < 0.05. GO terms were sorted in descending order of fold enrichment values.

To simplify the identification of devil MHC allotypes and maintain consistency in nomenclature to previous works, MHC transcripts in this manuscript were renamed according to Cheng et al., based on sequence similarity[45] (see **Supplementary Table 4** for corresponding NCBI gene symbols). MHC transcripts *LOC100918485* and *LOC100918744*, which have not been previously characterised, are predicted to encode beta chains of the MHC-II DA gene based on gene homology. These transcripts were renamed as *SAHA-DAB_X1* and *SAHA-DAB_X2*, respectively. Similarly, genes without an official gene symbol (LOC prefixes) were given aliases based on the gene description on NCBI.

2.5 Flow cytometric analysis of B2M and MHC-II expression

Cultured cells were harvested using TrypLE™ Express Enzyme (1X) (Thermo Fisher Scientific) and counted using a haemocytometer. 1×10^5 cells per well were aliquoted into round-bottom 96-well plates and washed with 1X PBS (Thermo Fisher Scientific). Washing steps include centrifugation at 500*g* for 3 min at 4 °C to pellet cells before removal of supernatant. Cells were first stained with Invitrogen™ LIVE/DEAD™ Fixable Near-IR Dead Cell Stain kit (Thermo Fisher Scientific) diluted according to manufacturer's instructions for 30 min on ice, protected from light. After staining, cells were washed twice with 1X PBS. For MHC-II expression, a monoclonal mouse antibody against the intracellular tail of human HLA-DR α chain was used (Clone TAL.1B5, # M0746, Agilent, Santa Clara, CA, USA). Detection of MHC-I on the surface of cells was performed using a monoclonal mouse antibody against devil beta-2-microglobulin (B2M) in supernatant (Clone 13-34-45; a gift from Hannah Siddle[5]). Cells for intracellular staining of HLA-DR were first fixed and permeabilised using BD Cytofix/Cytoperm™ Plus Fixation/Permeabilization Kit (BD Biosciences, North Ryde, NSW, Australia). All intracellular antibody staining, and washes were carried out in 1X BD Perm/Wash™ Buffer (BD Biosciences) while FACS buffer (PBS with 0.5% BSA, 0.02% sodium azide) was used for surface antibody staining. All cells were incubated with 1% normal goat serum (Thermo Fisher Scientific) for blocking, 10 min on ice. After that, cells were washed and incubated with either anti-human HLA-DRα (0.48 µg/mL) or anti-devil B2M antibody (1:250 v/v dilution) for 30 min on ice. Cells were washed once and stained with goat anti-mouse IgG-Alexa Fluor 488 (2 µg/mL, # A11029, Thermo Fisher Scientific) for 30 min on ice, in the dark. Two final washes were given to remove excess secondary antibody. Fixed cells were resuspended in FACS buffer while the rest were resuspended in FACS fix solution (0.02% sodium azide, 1.0% glucose, 0.4% formaldehyde). Analysis was carried out using Cytek™ Aurora (Cytek Biosciences, Fremont, CA, USA). As a positive control for MHC-I expression, DFT cells were treated with 10 ng/mL devil recombinant IFNG[46] for 24 h.

2.6 Protein extraction and western blot

Cells were harvested and centrifuged at 500*g* for 5 min at room temperature. The pellet was washed twice with cold 1X PBS and weighed. Total cell protein was extracted by adding 1 mL RIPA Lysis and Extraction Buffer (Thermo Fisher Scientific), 10 µL Halt™ Protease Inhibitor Cocktail (Thermo Fisher Scientific) and 10 µL Halt™ Phosphatase Inhibitor Cocktail (Thermo Fisher Scientific) per 40 mg of wet cell pellet. The suspension was sonicated for 30 seconds with 50% pulse and then mixed gently for 15 min on ice. The mixture was centrifuged at

14000*g* for 15 min to pellet the cell debris. The supernatant was transferred to a new tube and total protein was quantified using EZQ® Protein Quantitation kit (Invitrogen) according to manufacturer's instructions. Two replicates per cell line were prepared for protein extraction.

20 µg of protein per sample was used for target protein detection by western blot. Protein samples were subjected to SDS-PAGE using Bolt™ 4-12%, Bis-Tris, 1.0 mm Mini Protein Gel (Thermo Fisher Scientific). Briefly, protein samples were treated with 1X Bolt™ LDS Sample Buffer (Thermo Fisher Scientific) and 1X Bolt™ Reducing Agent (Thermo Fisher Scientific) at 70 °C for 10 min. Samples were loaded onto the gel and run with 1X Bolt™ MES SDS Running Buffer (Thermo Fisher Scientific) in the Mini Gel Tank (Thermo Fisher Scientific) at 100 V for 5 min followed by 200 V for 15 min. SeeBlue™ Plus2 Pre-stained Protein Standard (Thermo Fisher Scientific) was used as a molecular weight marker. Proteins were transferred to a nitrocellulose membrane using iBlot™ Transfer Stack, nitrocellulose, mini (Thermo Fisher Scientific) and iBlot™ Gel Transfer Device (Thermo Fisher Scientific) using the following settings: 20 V for 7.5 min.

For immunodetection, the membrane was blocked with TBSTM (Tris-buffered saline (TBS): 50 mM Tris-HCl, 150 mM NaCl, pH 7.6), 0.05% Tween 20, and 5% skim milk) for 1 hour at room temperature and rinsed twice with TBST (TBS, 0.05% Tween 20). Then, the membrane was incubated with: (i) rabbit polyclonal anti-beta actin antibody (# ab8227, Abcam, Cambridge, UK) diluted in TBSTM (400 ng/mL), (ii) mouse monoclonal anti-devil SAHA-UA/UB/UC in supernatant (Clone 15-25-18; a gift from Hannah Siddle[10]), or (iii) mouse monoclonal anti-devil SAHA-UK in supernatant (Clone 15-29-1; a gift from Hannah Siddle[10]) overnight at 4 °C. The membranes were washed four times with TBST for a duration of 5 min each wash. After that, the membranes were incubated with either HRP-conjugated goat anti-mouse (250 ng/mL; # P0447, Agilent) or HRP-conjugated goat anti-rabbit immunoglobulin (62.5 ng/mL; # P0448, Agilent) diluted in TBSTM for 1 hour at room temperature. The membranes were given final washes as described above. All incubation and washing steps were performed under agitation. Target protein expression was detected using Immobilon™ Western Chemiluminescent HRP Substrate (Merck Millipore, Burlington, MA, USA) according to manufacturer's protocol. Protein bands were visualised using Amersham™ Imager 600 (GE Healthcare Life Sciences, Malborough, MA, USA).

2.7 Flow cytometric analysis of serum antibody binding

Serum samples from four devils (My, TD4, TD5, and TD6), collected before (pre-immune) and after DFT1 clinical manifestations (immune), were used to assess antibody responses towards CIITA-expressing DFT cell lines (**Supplementary Table 5**). The serum samples were identified as immune from the presence of anti-DFT1 antibodies, which were found to be predominantly against MHC-I on DFT1 cells[8]. 'My' was a devil that was immunised, challenged with DFT1 cells, and subsequently treated with an experimental immunotherapy that induced tumour regression[9]. TD4, TD5, and TD6 were naturally DFT1-infected wild devils with either spontaneous tumour regressions (TD4); MHC-II$^+$ and CD3$^+$ tumour-infiltrating lymphocytes in the tumour (TD5); or B2M$^+$ DFT1 cells in fine needle aspirations of a tumour (TD6)[7]. A devil with no clinical signs of DFTD during serum collection (TD7) was included as a negative control for antibody binding towards the DFT cell lines.

Cells were harvested and aliquoted into round-bottom 96-well plates as indicated above. After washing with PBS, cells were stained with LIVE/DEAD™ Fixable Near-IR Dead Cell Stain for 30 min on ice and washed twice with PBS. For blocking, cells were incubated with 1% normal goat serum for 10 min and washed once with FACS buffer. Serum samples were thawed on ice and diluted with FACS buffer (1:50 v/v). 50 µL of serum was added to cells for 1 h and then washed. After that, cells were stained with 10 µg/mL monoclonal mouse anti-devil IgG antibody (A4-D1-2-1, provided by WEHI)[47] diluted in FACS buffer for 30 min. The cells were washed and stained with 2 µg/mL goat anti-mouse IgG-Alexa Fluor 647 (# A21235, Thermo Fisher Scientific) in FACS buffer for 30 min. After washing, cells were fixed in FACS fix solution and analysed on Cytek™ Aurora. All washing steps include two washes with FACS buffer unless indicated otherwise and all staining steps were carried out on ice, protected from light.

3. Results

3.1 CIITA plays a dominant role in antigen presentation

To delineate the role of CIITA in DFT cells, differentially expressed genes following stable expression of CIITA were analysed by gene ontology (GO) functional enrichment analysis. Differential expression analysis revealed 888 genes, excluding CIITA, that were modulated ($|\log_2 FC| \geq 2$, FDR < 0.05) in DFT1.CIITA compared to vector-only cell line DFT1.BFP (**Figure 1**, **Supplementary Table 3**). In DFT2.CIITA, there were 56 genes that were differentially expressed relative to DFT2.BFP. Ten genes were commonly up- or down-

regulated by CIITA in DFT1 and DFT2 cells. Most of these genes were of the MHC-II antigen processing and presentation pathway. *SAHA-DAA, SAHA-DAB2* and *SAHA-DAB3* are devil classical MHC-II genes while *SAHA-DMA* and *SAHA-DMB* encode non-classical MHC-II. Others include *CD74* and gamma-interferon-inducible lysosomal thiol reductase (*IFI30*), which encode the invariant chain, an MHC-II chaperone, and an enzyme for lysosomal degradation of proteins, respectively. Except for *IFI30*, these genes were among the most highly upregulated genes in the transcriptome of DFT1.CIITA (**Table 2**) and DFT2.CIITA (**Table 3**).

In DFT1.CIITA, several MHC-I heavy chain and accessory genes were strongly induced, depicting a role of CIITA in MHC-I antigen presentation (**Table 2**). These include: (i) MHC-I heavy alpha chain genes *SAHA-UA, SAHA-UB*, and *SAHA-UC*; and (ii) *B2M*, which associates with MHC-I alpha chains to form the trimeric structure of MHC-I molecules; (iii) transporter associated with antigen processing 1 (*TAP1*) for peptide transport into the endoplasmic reticulum; and (iv) proteasomal subunits *PSMB8* and *PSMB9*.

Next, all significantly up- or down-regulated genes were analysed for enriched GO biological processes using DAVID bioinformatics resource. Thresholds p value < 0.05 and FDR < 0.05 were applied to filter out insignificant over-represented GO terms. The most significantly enriched GO biological process in the list of upregulated genes in DFT1.CIITA and DFT2.CIITA was *antigen processing and presentation* (GO:0019882) followed by *immune response* (GO:0006955) (**Table 4**). Both processes were identified in genes of the MHC-I and MHC-II machinery (**Supplementary Tables 6** and **7**). C*ell adhesion* (GO:0007155) and *cell communication* (GO:0007154) were enriched in genes downregulated in DFT1.CIITA; there were no GO biological processes that were associated with downregulated genes in DFT2.CIITA.

3.2 Regulation of MHC-I and MHC-II pathway by CIITA

To further characterise the regulation of MHC-I and MHC-II by CIITA and how it differs from IFNG or NLRC5 stimulation, a heatmap was used to display the relative expression of MHC-I and MHC-II genes, and key accessory proteins between the different treatments. The transcriptome of IFNG-treated DFT2 cells was previously carried out on DFT2 cell line RV (DFT2.WT^{RV})[27] while subsequent experiments on DFT2 cells were performed using DFT2 cell line JV (DFT2.WT). Schwann cell differentiation marker SRY-box 10 (*SOX10*) and

neuroepithelial marker nestin (*NES*) were used as internal gene controls, and myelin protein periaxin (*PRX*) was used to discriminate DFT1 cells from DFT2.

As described above, CIITA induced the transcription of *B2M;* MHC-I heavy chains *SAHA-UA*, *-UB*, *-UC*; *PSBM8; PSMB9;* and *TAP1* in DFT1 cells. There was also an upregulation of non-classical MHC-I *SAHA-UK*, and downregulation of *NLRC5* and proteasomal subunit *PSBM10* in DFT1.CIITA cells (**Figure 2**). Excluding *NLRC5*, genes that were modulated in DFT1.CIITA were synonymously up- or down-regulated in DFT1.NLRC5, suggesting similar roles of CIITA to NLRC5 in DFT1 cells. However, induction of the MHC-I pathway by CIITA was not as strong as NLRC5 despite having similarly high levels of expression in the respective cell lines (**Figure 2**, **Supplementary Table 3**). IFNG exhibited a wider range in regulation of genes from the MHC-I pathway compared to NLRC5 and CIITA. Peptide transporter *TAP2* and MHC-I chaperone TAP binding protein (*TAPBP*) were exclusively upregulated by IFNG in DFT1 and DFT2 cells. Meanwhile, the expression of CIITA in DFT2 cells did not appear to significantly influence any of the MHC-I machinery.

High levels of CIITA transcripts in DFT1.CIITA was correlated with strong induction of all the MHC-II genes, with *SAHA-DAB_X1* and *SAHA-DAB_X2* being the weakest. This was not observed in the other cell lines nor in DFT2.CIITA. CIITA was expressed to a lesser extent in DFT2.CIITA relative to DFT1.CIITA, and all MHC-II genes but *SAHA-DAB_X1* and *SAHA-DAB_X2* were upregulated. The expression of *CIITA*, MHC-II genes and *CD74* was relatively low in DFT1.WT and DFT2.WT cells except for *SAHA-DAB2* and *SAHA-DAB3* in DFT1.WT. There was a moderate increase in CIITA expression after IFNG treatment in DFT1 cells, but it was insufficient to initiate transcription of MHC-II genes or *CD74*. In IFNG-treated DFT2 cells where CIITA was induced to a higher degree, there was only partial activation of the MHC-II gene set (*SAHA-DAA*, *SAHA-DMA*, *SAHA-DMB*), and an upregulation of *CD74*. Interestingly, MHC-II protease cathepsin *CTSS* was only induced with IFNG treatment in DFT1 and DFT2 cells.

3.3 MHC-I and MHC-II molecules are upregulated by CIITA in DFT cells

MHC-II (HLA-DRA) protein expression was absent in wild type (WT) DFT1 and DFT2 cells and in vector-only transfected cells (BFP) but was significantly upregulated in CIITA-expressing DFT1 cells (**Figure 3A**). In DFT2 cells, the overexpression of CIITA did not alter median MHC-II expression, or more specifically MHC-II gene loci HLA-DRA. Neither IFNG treatment nor NLRC5 overexpression induced MHC-II protein expression in DFT1 and DFT2

cells. CIITA was capable of restoring surface expression of B2M in DFT1 cells, albeit to a lesser degree than NLRC5 and IFNG stimulation, consistent with the transcriptomic results (**Figure 3A**, **Figure 2**). Meanwhile the basal expression of B2M in DFT2 cells was enhanced slightly by CIITA.

In agreement with an increase in surface B2M expression on DFT1.CIITA by flow cytometry, an upregulation of MHC-I heavy chains was detected by western blot compared to wild type (DFT1.WT) and vector-only cells (DFT1.BFP) (**Figure 3B**). IFNG-treated and NLRC5-overexpressing DFT1 and DFT2 cells also expressed elevated levels of MHC-I heavy chains. Although flow cytometry detected an increase in B2M expression on DFT2.CIITA, the expression of MHC-I heavy chains by western blot was similar to DFT2.WT and DFT2.BFP.

3.4 Analysis of anti-DFT serum antibody response against CIITA-induced antigens

We have previously shown that MHC-I on DFT1 cells is the predominant antibody target in devils with natural and induced anti-DFT immune response including tumour regressions[8]. Here we tested if expression of CIITA in DFT cells could also upregulate antibody targets on DFT cells. Four devils (My, TD4, TD5, TD6) that developed DFT1 tumours and subsequent serum antibodies (immune) that bound MHC-I were selected for screening against CIITA-expressing DFT1 and DFT2 cells. Serum from each devil prior to DFT1 infection or observable DFT1 tumours (pre-immune) was included to assess the change in antibody levels after DFT1 infection.

Relative to MHC-I negative DFT1.WT and DFT1.BFP, serum antibodies from all four devils post-DFT1 development generally showed higher binding to DFT1 cells overexpressing NLRC5 (**Figure 4**). Antibody levels against CIITA-expressing DFT1 cells were higher than DFT1.WT and DFT1.BFP in immune sera from My, a captive devil with an immunotherapy-induced DFT1 regression, and TD4, a wild devil with a natural DFT1 regression. Binding of serum antibodies to DFT1.CIITA cells was relatively lower than DFT1.NLRC5. There was no increase in antibody binding towards DFT1.CIITA compared to DFT1.WT and DFT1.BFP from immune sera of devils TD5 and TD6.

Serum from DFT1-infected devils reacted with DFT2 cells but only following NLRC5 overexpression. Serum from My, TD4, TD5 and TD6 all had strong antibody binding to DFT2.NLRC5 which was not observed in the other DFT2 cell lines. This suggests that NLRC5 upregulates similar antigenic target(s) in DFT1 and DFT2 cells.

4. Discussion

Clonally transmissible cancers in nature are rare, and yet the Tasmanian devils are affected by two of the only three known naturally occurring transmissible cancers in vertebrates. In a cancer where allogeneity exists between individual host tissues and tumour, allogeneic MHC molecules on tumour cells are important targets for anti-tumour immunity. MHC-I expression on DFT1 cells has been exploited for vaccine development and immunotherapy to enhance anti-DFT immunity via $CD8^+$ T cell responses[9]. In this study, we showed that the class II transactivator CIITA can modulate MHC-I and MHC-II antigen processing and presentation pathways in DFT cells. Surprisingly, the overexpression of CIITA resulted in upregulation of MHC-I and MHC-II molecules in DFT1 cells but not DFT2 cells.

MHC-II expression is normally confined to a subset of haematopoietic antigen-presenting cells, and DFT1 and DFT2 cells do not typically express MHC-II genes and proteins. We demonstrated the expression of MHC-II proteins in non-haematopoietic DFT1 cells through CIITA-induced upregulation of classical and non-classical MHC-II genes, and the invariant chain *CD74*. The lack of detectable MHC-II proteins in CIITA-expressing DFT2 cells could be due to insufficient expression of MHC-II genes and *CD74* for stable expression of MHC-II molecules. Post-transcriptional regulation might be involved in MHC-II expression in DFT cells, as described in human T cells[48]. However, the regulation of MHC-II expression by CIITA in a quantitative (and qualitative) manner, in which CIITA is the rate-determining factor for mRNA and protein expression of MHC-II genes[49], suggests a correlation between lack of MHC-II protein expression and the relatively low CIITA expression in DFT2.CIITA compared to DFT1.CIITA. A heterozygous non-synonymous mutation (D59N) in transcription factor *RFX5* is present in DFT2 tumours[6]. RFX5 is a transcription factor of the multiprotein MHC enhanceosome that regulates MHC-I and MHC-II expression[50,51]. Although transcription of MHC-I and MHC-II genes were inducible in DFT2 cells following stimulation, the functional impact of this mutation on MHC transcription remains to be explored.

Differential expression of MHC-II allotypes upon CIITA induction, as observed with *SAHA-DAB_X1* and *SAHA-DAB_X2* that were consistently expressed at lower levels compared to other MHC-II genes, suggests additional regulatory mechanism(s) that control the expression of MHC-II genes beyond that of CIITA. Variations in expression levels of MHC-I and MHC-II genes have been associated with sequence polymorphism in the promoter or 3' untranslated region (UTR) of MHC genes, which modulates transcription either epigenetically or non-

414 epigenetically, in addition to post-transcriptional regulation[52–54]. The varying degrees of
415 inducibility and expression of devil MHC-II allotypes could correlate to tissue-specific
416 expression, with functions that differ from classical MHC-II genes.

417 Consistent with findings from pioneering studies on CIITA function[20,21], CIITA exhibited
418 transcriptional activity over the MHC-I pathway in DFT1 cells that lack MHC-I expression.
419 The ability of CIITA to regulate MHC-I expression is attributed to similarities in the regulatory
420 elements at the proximal promoters of MHC-I and MHC-II genes, and interaction with the
421 same transcription factors of the MHC enhanceosome as NLRC5[20,21,51,55,56]. In MHC-I positive
422 DFT2 cells, overexpression of CIITA resulted in minimal upregulation of MHC-I compared
423 with NLRC5 or IFNG stimulation. The limited CIITA influence on MHC-I expression is
424 commonly observed in cells with high constitutive levels of MHC-I[20,21]. This illustrates the
425 role of NLRC5 as the primary transactivator for MHC-I expression and a secondary role for
426 CIITA.

427 Unlike the ubiquitous expression of MHC-I molecules in nucleated cells, MHC-II expression
428 is tightly regulated in a cell type-, differentiation-, and stimulus-specific manner. Evidence for
429 inducibility of MHC-II expression in DFT cells suggests that MHC-II-restricted tumour
430 antigen presentation could occur in the physiological setting under inflammatory conditions
431 that upregulate CIITA. This could provide additional targets for allogeneic antibody responses,
432 as our results show that CIITA upregulation increases binding of serum antibodies collected
433 from devils that had both natural and immunotherapy-induced DFT1 regressions. In canine
434 transmissible venereal tumour (CTVT), the tumour regression phase is often associated with
435 upregulation of MHC-I and MHC-II molecules, mediated by factors such as IFNG from tumour
436 infiltrating lymphocytes[57,58].

437 The capacity to express MHC-II molecules with CIITA expression could stem from the
438 Schwann cell origins of DFT1 and DFT2 cells[27,59]. Schwann cells express MHC-II molecules
439 upon traumatic and inflammatory injury, playing a role in antigen presentation to $CD4^+$ T cells
440 to modulate local immune responses[60,61]. Similarly, CIITA-expressing DFT cells have the
441 potential to present MHC-II-restricted tumour antigens to $CD4^+$ T cells and potentiate anti-
442 DFT immune responses. Several studies in murine models have demonstrated immune-
443 mediated tumour rejection and/or tumour growth retardation using MHC-II-expressing tumour
444 cell lines, either through CIITA or MHC-II gene transfer[62–67]. These primary responses were
445 also protective against subsequent challenge with parental MHC-II negative tumours. The

expression of MHC-II on CIITA-expressing DFT cells can offer insight into the importance of $CD4^+$ T cells in the interplay with other immune cells for anti-tumour immunity and allograft rejection.

In this study, the role of CIITA as the master regulator of MHC-II expression was reaffirmed in a non-model immunology research species. We have delineated the regulation of MHC-I and MHC-II pathways by CIITA in marsupials and transmissible cancers. The ability to induce MHC-II expression in transmissible tumour cells creates an avenue for vaccine and immunotherapeutic strategies to enhance anti-tumour immunity through $CD4^+$ T cell help and inform of the importance of MHC-II in anti-tumour and allogeneic immune responses. The relatively simple process we developed for making cell lines that constitutively express NLRC5 and CIITA can be readily adapted for many other species and potentially be used in conjunction with CD80/CD86 to provide antigen stimulation in *in vitro* assays. This is critical for 99% of species that lack reagents, such as agonistic anti-CD3 and anti-CD28 antibodies, for inducing T cell activation *in vitro*.

Declaration of competing interest

The authors declare that the research was conducted in the absence of any commercial or financial relationships that could be construed as a potential conflict of interest.

Funding

This work was supported by the Australian Research Council (ARC) DECRA grant # DE180100484 and ARC Discovery grant # DP180100520, University of Tasmania Foundation Dr. Eric Guiler Tasmanian Devil Research Grant through funds raised by the Save the Tasmanian Devil Appeal (2013, 2015, 2017).

Authors' contributions

ABL, ASF, CEBO and GMW designed the study. ASF and CEBO developed the technology. CEBO performed the experiments and bioinformatic analyses. CEBO created the figures. ABL, ASF, CEBO, GMW, HVS and YC analysed and interpreted the data. CEBO wrote the manuscript, and all authors edited the manuscript.

Acknowledgements

The authors would like to thank Jocelyn Darby and Alana De Luca for assistance in the lab, Terry Pinfold for assistance in flow cytometry, and Amanda Patchett for assistance in bioinformatic analysis. We wish to thank G. Ralph for ongoing care of Tasmanian devils, the

Bonorong Wildlife Sanctuary for providing access to Tasmanian devils, and R. Pye for providing care for devils and collecting blood samples.

References

1 Cunningham CX, Comte S, McCallum H, Hamilton DG, Hamede R, Storfer A *et al.* Quantifying 25 years of disease-caused declines in Tasmanian devil populations: host density drives spatial pathogen spread. *Ecol Lett* 2021; **24**: 958–969.

2 Pearse A-M, Swift K. Allograft theory: Transmission of devil facial-tumour disease. *Nature* 2006; **439**: 549.

3 Pye RJ, Pemberton D, Tovar C, Tubio JMC, Dun KA, Fox S *et al.* A second transmissible cancer in Tasmanian devils. *Proc Natl Acad Sci U S A* 2016; **113**: 374–379.

4 Siddle H V, Kreiss A, Eldridge MDB, Noonan E, Clarke CJ, Pyecroft S *et al.* Transmission of a fatal clonal tumor by biting occurs due to depleted MHC diversity in a threatened carnivorous marsupial. *Proc Natl Acad Sci U S A* 2007; **104**: 16221–6.

5 Siddle H V, Kreiss A, Tovar C, Yuen CK, Cheng Y, Belov K *et al.* Reversible epigenetic down-regulation of MHC molecules by devil facial tumour disease illustrates immune escape by a contagious cancer. *Proc Natl Acad Sci U S A* 2013; **110**: 5103–5108.

6 Stammnitz MR, Coorens THH, Gori KC, Hayes D, Fu B, Wang J *et al.* The Origins and Vulnerabilities of Two Transmissible Cancers in Tasmanian Devils. *Cancer Cell* 2018; **33**: 607-619.e15.

7 Pye R, Hamede R, Siddle H V., Caldwell A, Knowles GW, Swift K *et al.* Demonstration of immune responses against devil facial tumour disease in wild Tasmanian devils. *Biol Lett* 2016; **12**: 20160553.

8 Ong CEB, Patchett AL, Darby JM, Chen J, Liu G-S, Lyons AB *et al.* NLRC5 regulates expression of MHC-I and provides a target for anti-tumor immunity in transmissible cancers. *J Cancer Res Clin Oncol* 2021; : 1–19.

9 Tovar C, Pye RJ, Kreiss A, Cheng Y, Brown GK, Darby J *et al.* Regression of devil facial tumour disease following immunotherapy in immunised Tasmanian devils. *Sci Rep* 2017; **7**: 43827.

10 Caldwell A, Coleby R, Tovar C, Stammnitz MR, Kwon YM, Owen RS *et al.* The newly-arisen Devil facial tumour disease 2 (DFT2) reveals a mechanism for the emergence of a contagious cancer. *Elife* 2018; **7**: e35314.

11 Hung K, Hayashi R, Lafond-Walker A, Lowenstein C, Pardoll D, Levitsky H. The central role of CD4+ T cells in the antitumor immune response. *J Exp Med* 1998; **188**: 2357–2368.

12 Janssen EM, Lemmens EE, Wolfe T, Christen U, Von Herrath MG, Schoenberger SP. CD4+ T cells are required for secondary expansion and memory in CD8+ T lymphocytes. *Nature* 2003; **421**: 852–856.

13 Kumamoto Y, Mattei LM, Sellers S, Payne GW, Iwasaki A. CD4+ T cells support cytotoxic T lymphocyte priming by controlling lymph node input. *Proc Natl Acad Sci U S A* 2011; **108**: 8749–8754.

14 Bennett SRM, Carbone FR, Karamalis F, Flavell RA, Miller JFAP, Heath WR. Help for cytotoxic-T-cell responses is mediated by CD4O signalling. *Nature* 1998; **393**: 478–480.

15 Dalloul AH, Chmouzis E, Ngo K, Fung-Leung WP. Adoptively transferred CD4+ lymphocytes from CD8 -/- mice are sufficient to mediate the rejection of MHC class II or class I disparate skin grafts. *J Immunol* 1996; **156**: 4114–4119.

16 Krieger NR, Yin DP, Fathman CG. CD4+ but not CD8+ cells are essential for allorejection. *J Exp Med* 1996; **184**: 2013–2018.

17 Propper DJ, Chao D, Braybrooke JP, Bahl P, Thavasu P, Balkwill F *et al.* Low-Dose IFN-γ Induces Tumor MHC Expression in Metastatic Malignant Melanoma. *Clin Cancer Res* 2003; **9**: 84–92.

18 Steimle V, Otten LA, Zufferey M, Mach B. Complementation cloning of an MHC class II transactivator mutated in hereditary MHC class II deficiency (or bare lymphocyte syndrome). *Cell* 1993; **75**: 135–146.

19 Steimle V, Siegrist CA, Mottet A, Lisowska-Grospierre B, Mach B. Regulation of MHC class II expression by interferon-γ mediated by the transactivator gene CIITA. *Science (80-)* 1994; **265**: 106–109.

20 Gobin SJP, Peijnenburg A, Keijsers V, Van Den Elsen PJ. Site α is crucial for two routes of IFNγ-induced MHC class I transactivation: the ISRE-mediated route and a novel pathway involving CIITA. *Immunity* 1997; **6**: 601–611.

21 Martin BK, Chin KC, Olsen JC, Skinner CA, Dey A, Ozato K *et al.* Induction of MHC class I expression by the MHC class II transactivator CIITA. *Immunity* 1997; **6**: 591–600.

22 Pearse A-M, Swift K, Hodson P, Hua B, McCallum H, Pyecroft S *et al.* Evolution in a transmissible cancer: a study of the chromosomal changes in devil facial tumor (DFT) as it spreads through the wild Tasmanian devil population. *Cancer Genet* 2012; **205**: 101–112.

23 Kowarz E, Löscher D, Marschalek R. Optimized Sleeping Beauty transposons rapidly generate stable transgenic cell lines. *Biotechnol J* 2015; **10**: 647–653.

24 Flies AS, Darby JM, Murphy PR, Pinfold TL, Patchett AL, Lennard PR. Generation and Testing of Fluorescent Adaptable Simple Theranostic (FAST) Proteins. *Bio-protocol* 2020; **10**: e3696.

25 Mátés L, Chuah MKL, Belay E, Jerchow B, Manoj N, Acosta-Sanchez A *et al.* Molecular evolution of a novel hyperactive Sleeping Beauty transposase enables robust stable gene transfer in vertebrates. *Nat Genet* 2009; **41**: 753–761.

26 Patchett AL, Wilson R, Charlesworth JC, Corcoran LM, Papenfuss AT, Lyons BA *et al.* Transcriptome and proteome profiling reveals stress-induced expression signatures of imiquimod-treated Tasmanian devil facial tumor disease (DFTD) cells. *Oncotarget* 2018; **9**: 15895–15914.

27 Patchett AL, Coorens THH, Darby J, Wilson R, McKay MJ, Kamath KS *et al.* Two of a kind: transmissible Schwann cell cancers in the endangered Tasmanian devil (*Sarcophilus harrisii*). *Cell Mol Life Sci* 2020; **77**: 1847–1858.

28 Andrews S. FastQC: A Quality Control tool for High Throughput Sequence Data. 2010. doi:https://www.bioinformatics.babraham.ac.uk/projects/fastqc/.

29 Liao Y, Smyth GK, Shi W. The Subread aligner: fast, accurate and scalable read mapping by seed-and-vote. *Nucleic Acids Res* 2013; **41**: e108–e108.

30 Liao Y, Smyth GK, Shi W. featureCounts: an efficient general purpose program for assigning sequence reads to genomic features. *Bioinformatics* 2014; **30**: 923–930.

31 RStudio Team. RStudio: Integrated Development Environment for R. 2020.http://www.rstudio.com/.

32 R Core Team. R: A Language and Environment for Statistical Computing. 2020.https://www.r-project.org/.

33 Robinson MD, McCarthy DJ, Smyth GK. edgeR: A Bioconductor package for differential expression analysis of digital gene expression data. *Bioinformatics* 2009; **26**: 139–140.

34 Robinson MD, Oshlack A. A scaling normalization method for differential expression analysis of RNA-seq data. *Genome Biol* 2010; **11**: R25.

35 Anders S, Huber W. Differential expression analysis for sequence count data. *Genome Biol* 2010; **11**: R106.

36 Bullard JH, Purdom E, Hansen KD, Dudoit S. Evaluation of statistical methods for normalization and differential expression in mRNA-Seq experiments. *BMC Bioinformatics* 2010; **11**: 94.

37 Risso D, Schwartz K, Sherlock G, Dudoit S. GC-Content Normalization for RNA-Seq Data. *BMC Bioinformatics* 2011; **12**: 480.

38 Law CW, Chen Y, Shi W, Smyth GK. voom: Precision weights unlock linear model analysis tools for RNA-seq read counts. *Genome Biol* 2014; **15**: R29.

39 Ritchie ME, Phipson B, Wu D, Hu Y, Law CW, Shi W *et al. limma* powers differential expression analyses for RNA-sequencing and microarray studies. *Nucleic Acids Res* 2015; **43**: e47.

40 Phipson B, Lee S, Majewski IJ, Alexander WS, Smyth GK. Robust hyperparameter estimation protects against hypervariable genes and improves power to detect differential expression. *Ann Appl Stat* 2016; **10**: 946–963.

41 Oliveros JC. Venny. An interactive tool for comparing lists with Venn's diagrams. 2015.https://bioinfogp.cnb.csic.es/tools/venny/index.html.

42 Gu Z, Eils R, Schlesner M. Complex heatmaps reveal patterns and correlations in multidimensional genomic data. *Bioinformatics* 2016; **32**: 2847–2849.

43 Huang DW, Sherman BT, Lempicki RA. Bioinformatics enrichment tools: Paths toward the comprehensive functional analysis of large gene lists. *Nucleic Acids Res* 2009; **37**: 1–13.

44 Huang DW, Sherman BT, Lempicki RA. Systematic and integrative analysis of large gene lists using DAVID bioinformatics resources. *Nat Protoc* 2009; **4**: 44–57.

45 Cheng Y, Stuart A, Morris K, Taylor R, Siddle H, Deakin J *et al.* Antigen-presenting genes and genomic copy number variations in the Tasmanian devil MHC. *BMC Genomics* 2012; **13**: 87.

46 Flies AS, Lyons AB, Corcoran LM, Papenfuss AT, Murphy JM, Knowles GW *et al.* PD-L1 is not constitutively expressed on Tasmanian devil facial tumor cells but is strongly upregulated in response to IFN-γ and can be expressed in the tumor

microenvironment. *Front Immunol* 2016; **7**: 581.

47 Howson LJ, Morris KM, Kobayashi T, Tovar C, Kreiss A, Papenfuss AT *et al.* Identification of dendritic cells, B cell and T cell subsets in Tasmanian devil lymphoid tissue; evidence for poor immune cell infiltration into devil facial tumors. *Anat Rec (Hoboken)* 2014; **297**: 925–938.

48 Caplen HS, Salvadori S, Gansbacher B, Zier KS. Post-transcriptional regulation of MHC class II expression in human T cells. *Cell Immunol* 1992; **139**: 98–107.

49 Otten LA, Steimle V, Bontron S, Mach B. Quantitative control of MHC class II expression by the transactivator CIITA. *Eur J Immunol* 1998; **28**: 473–478.

50 Gobin SJP, Peijnenburg A, Van Eggermond M, Van Zutphen M, Van Den Berg R, Van Den Elsen PJ. The RFX complex is crucial for the constitutive and CIITA-mediated transactivation of MHC class I and β_2-microglobulin genes. *Immunity* 1998; **9**: 531–541.

51 Masternak K, Muhlethaler-Mottet A, Villard J, Zufferey M, Steimle V, Reith W. CIITA is a transcriptional coactivator that is recruited to MHC class II promoters by multiple synergistic interactions with an enhanceosome complex. *Genes Dev* 2000; **14**: 1156–1166.

52 Leen MPJM, Gorski J. Differential expression of isomorphic HLA-DRβ genes is not a sole function of transcription. *Hum Immunol* 1996; **50**: 111–120.

53 Kulkarni S, Savan R, Qi Y, Gao X, Yuki Y, Bass SE *et al.* Differential microRNA regulation of HLA-C expression and its association with HIV control. *Nature* 2011; **472**: 495–498.

54 Andersen LC, Beaty JS, Nettles JW, Seyfried CE, Nepom GT, Nepom BS. Allelic polymorphism in transcriptional regulatory regions of HLA-DQB genes. *J Exp Med* 1991; **173**: 181–192.

55 Gobin SJP, van Zutphen M, Westerheide SD, Boss JM, van den Elsen PJ. The MHC-specific enhanceosome and its role in MHC class I and β_2-microglobulin gene transactivation. *J Immunol* 2001; **167**: 5175–5184.

56 Meissner TB, Liu Y-J, Lee K-H, Li A, Biswas A, van Eggermond MCJA *et al.* NLRC5 cooperates with the RFX transcription factor complex to induce MHC class I gene expression. *J Immunol* 2012; **188**: 4951–4958.

57 Hsiao YW, Liao KW, Hung SW, Chu RM. Effect of tumor infiltrating lymphocytes on the expression of MHC molecules in canine transmissible venereal tumor cells. *Vet Immunol Immunopathol* 2002; **87**: 19–27.

58 Hsiao Y-W, Liao K-W, Chung T-F, Liu C-H, Hsu C-D, Chu R-M. Interactions of host IL-6 and IFN-γ and cancer-derived TGF-β1 on MHC molecule expression during tumor spontaneous regression. *Cancer Immunol Immunother* 2008; **57**: 1091–1104.

59 Murchison EP, Tovar C, Hsu A, Bender HS, Kheradpour P, Rebbeck CA *et al.* The Tasmanian devil transcriptome reveals Schwann cell origins of a clonally transmissible cancer. *Science* 2010; **327**: 84–87.

60 Meyer zu Hörste G, Heidenreich H, Lehmann HC, Ferrone S, Hartung HP, Wiendl H *et al.* Expression of antigen processing and presenting molecules by Schwann cells in inflammatory neuropathies. *Glia* 2010; **58**: 80–92.

61 Meyer zu Hörste G, Heidenreich H, Mausberg AK, Lehmann HC, ten Asbroek

ALMA, Saavedra JT *et al.* Mouse Schwann cells activate MHC class I and II restricted T-cell responses, but require external peptide processing for MHC class II presentation. *Neurobiol Dis* 2010; **37**: 483–490.

62 Meazza R, Comes A, Orengo AM, Ferrini S, Accolla RS. Tumor rejection by gene transfer of the MHC class II transactivator in murine mammary adenocarcinoma cells. *Eur J Immunol* 2003; **33**: 1183–1192.

63 Mortara L, Frangione V, Castellani P, De Lerma Barbaro A, Accolla RS. Irradiated CIITA-positive mammary adenocarcinoma cells act as a potent anti-tumor-preventive vaccine by inducing tumor-specific $CD4^+$ T cell priming and $CD8^+$ T cell effector functions. *Int Immunol* 2009; **21**: 655–665.

64 Frangione V, Mortara L, Castellani P, De Lerma Barbaro A, Accolla RS. CIITA-driven MHC-II positive tumor cells: Preventive vaccines and superior generators of antitumor $CD4^+$ T lymphocytes for immunotherapy. *Int J Cancer* 2010; **127**: 1614–1624.

65 Ekkirala CR, Cappello P, Accolla RS, Giovarelli M, Romero I, Garrido C *et al.* Class II Transactivator-Induced MHC Class II Expression in Pancreatic Cancer Cells Leads to Tumor Rejection and a Specific Antitumor Memory Response. *Pancreas* 2014; **43**: 1066–1072.

66 Ostrand-Rosenberg S, Clements VK, Thakur A, Cole GA. Transfection of major histocompatibility complex class I and class II genes causes tumour rejection. *Int J Immunogenet* 1989; **16**: 343–349.

67 Ostrand-Rosenberg S, Thakur A, Clements V. Rejection of mouse sarcoma cells after transfection of MHC class II genes. *J Immunol* 1990; **144**: 4068–4071.

Tables

Table 1. List of all devil facial tumour (DFT) cell lines and treatments

ID #	Sample name	Parent cell line	Treatment	References	ENA project #
1	DFT1.WT	DFT1 C5065	Untreated	Patchett et al., (2018)	PRJNA416378
2	DFT2.WT^{RV}	DFT2 RV	Untreated	Patchett et al., (2020)	PRJEB28680
3	DFT2.WT	DFT2 JV	Untreated	Ong et al., (2021)	PRJEB39847
4	DFT1.WT + IFNG	DFT1 C5065	5 ng/mL IFNG, 24h	Ong et al., (2021)	PRJEB39847
5	DFT2.WT^{RV} + IFNG	DFT2 RV	5 ng/mL IFNG, 24h	Ong et al., (2021)	PRJEB39847
6	DFT1.BFP	DFT1 C5065	Transfected with empty vector pSBbi-BH	Ong et al., (2021)	PRJEB39847
7	DFT2.BFP	DFT2 JV	Transfected with empty vector pSBbi-BH	Ong et al., (2021)	PRJEB39847
8	DFT1.NLRC5	DFT1 C5065	Transfected with NLRC5 vector pCO1	Ong et al., (2021)	PRJEB39847
9	DFT2.NLRC5	DFT2 JV	Transfected with NLRC5 vector pCO1	Ong et al., (2021)	PRJEB39847
10	DFT1.CIITA	DFT1 C5065	Transfected with CIITA vector pCO2	This study	PRJEB45867
11	DFT2.CIITA	DFT2 JV	Transfected with CIITA vector pCO2	This study	PRJEB45867

676 Table 2. Top 20 most significantly upregulated genes in DFT1.CIITA

Gene	**Gene description**	**MHC pathway**	**log_2FC**	**FDR**
SAHA-DAA	Class II histocompatibility antigen, DA alpha chain	Class II	17.09	1.90E-04
CD74	CD74 molecule	Class II	16.39	7.77E-05
CIITA	Class II major histocompatibility complex transactivator	Class II	15.40	1.07E-04
SAHA-DMB	Class II histocompatibility antigen, DM beta chain	Class II	10.26	7.00E-05
SAHA-DAB_X2	Class II histocompatibility antigen, DA beta chain	Class II	9.04	1.11E-03
SAHA-DAB_X1	Class II histocompatibility antigen, DA beta chain	Class II	8.82	7.77E-04
PSMB9	Proteasome 20S subunit beta 9	Class I	8.52	4.08E-04
SAHA-DMA	Class II histocompatibility antigen, DM alpha chain	Class II	6.52	5.12E-04
TAP1	Transporter 1, ATP binding cassette subfamily B member	Class I	6.46	6.95E-04
PSMB8	Proteasome 20S subunit beta 8	Class I	6.13	1.29E-03
SAHA-DAB3	Class II histocompatibility antigen, DA beta chain	Class II	6.08	7.72E-05
SAHA-UC	Class I histocompatibility antigen heavy chain	Class I	5.08	2.17E-03
SAHA-UA	Class I histocompatibility antigen heavy chain	Class I	4.77	2.29E-03
B2M	Beta-2-microglobulin	Class I	4.43	1.96E-05
SAHA-UB	Class I histocompatibility antigen heavy chain	Class I	4.41	2.25E-03
SAHA-DAB2	Class II histocompatibility antigen, DA beta chain	Class II	4.21	1.96E-05
ICOSLG	Inducible T Cell Costimulator (ICOS) Ligand	Unrelated	3.98	1.14E-03
KIF6	Kinesin family member 6	Unrelated	3.88	1.10E-02
BARX1	BARX homeobox 1	Unrelated	3.68	4.99E-03
MID1	Midline 1	Unrelated	3.67	3.52E-03

*See **Supplementary Table 3** full list of differentially expressed genes and log_2TPM values.*

677

678 Table 3. Significantly upregulated genes in DFT2.CIITA

Gene	**Gene description**	**MHC pathway**	**log_2FC**	**FDR**
CD74	CD74 molecule	Class II	13.60	6.69E-03
CIITA	Class II major histocompatibility complex transactivator	Class II	11.50	2.31E-03
SAHA-DAA	Class II histocompatibility antigen, DA alpha chain	Class II	8.52	2.31E-03
SAHA-DMB	Class II histocompatibility antigen, DM beta chain	Class II	8.34	2.81E-04
SAHA-DAB3	Class II histocompatibility antigen, DA beta chain	Class II	7.09	2.19E-03
SAHA-DMA	Class II histocompatibility antigen, DM alpha chain	Class II	6.82	6.82E-04
SAHA-DAB2	Class II histocompatibility antigen, DA beta chain	Class II	4.14	3.10E-04
BTN2A2	Butyrophilin subfamily 2 member A2	Unrelated	3.49	3.54E-02
NDUFA4L2	NDUFA4 mitochondrial complex associated like 2	Unrelated	2.83	2.72E-02

*See **Supplementary Table 3** full list of differentially expressed genes and log_2TPM values.*

679

680 Table 4. GO biological processes enriched in differentially expressed genes in DFT1.CIITA
681 and DFT2.CIITA

GO ID	GO term	Count	Term size	Fold enrichment	*p* value	FDR
DFT1.CIITA						
Upregulated						
GO:0019882	antigen processing and presentation	8	42	86.09	1.34E-12	1.19E-09
GO:0006955	immune response	9	518	7.85	4.75E-06	2.12E-03
Downregulated						
GO:0007155	cell adhesion	44	719	2.14	2.27E-06	4.48E-03
GO:0022610	biological adhesion	44	721	2.13	2.44E-06	4.48E-03
GO:0023052	signaling	113	2746	1.44	4.94E-06	6.05E-03
GO:0044700	single organism signaling	111	2726	1.42	1.12E-05	1.02E-02
GO:0007154	cell communication	112	2773	1.41	1.46E-05	1.07E-02
DFT2.CIITA						
Upregulated						
GO:0019882	antigen processing and presentation	4	42	215.21	9.33E-08	3.90E-05
GO:0006955	immune response	4	518	17.45	1.87E-04	3.91E-02

682

Figures

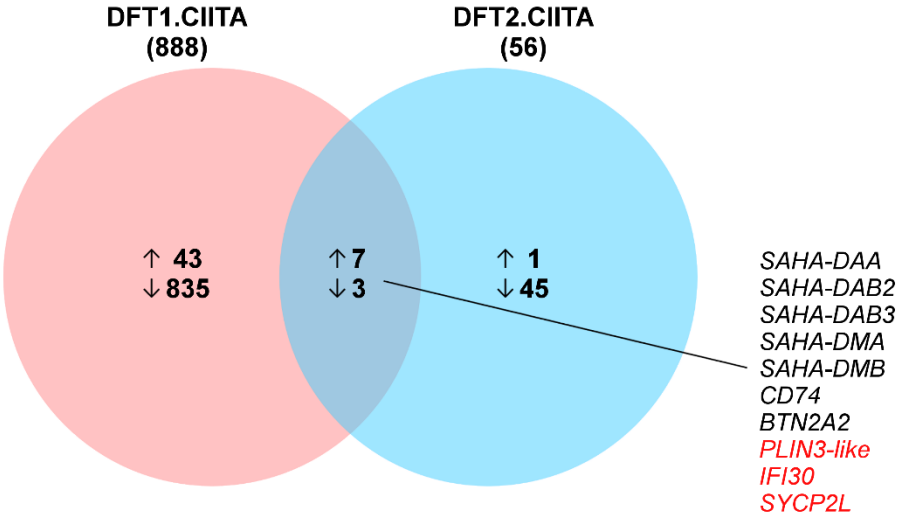

Figure 1. Venn diagram of differentially expressed genes in DFT1 and DFT2 cells with CIITA overexpression. Change in gene expression was identified between DFT.CIITA and vector-only control DFT.BFP. Total number of DEGs is indicated in parenthesis under sample name and the number of upregulated (↑) and downregulated genes (↓) are described in each Venn circle. Mutually inclusive genes that were upregulated are indicated in black and downregulated in red.

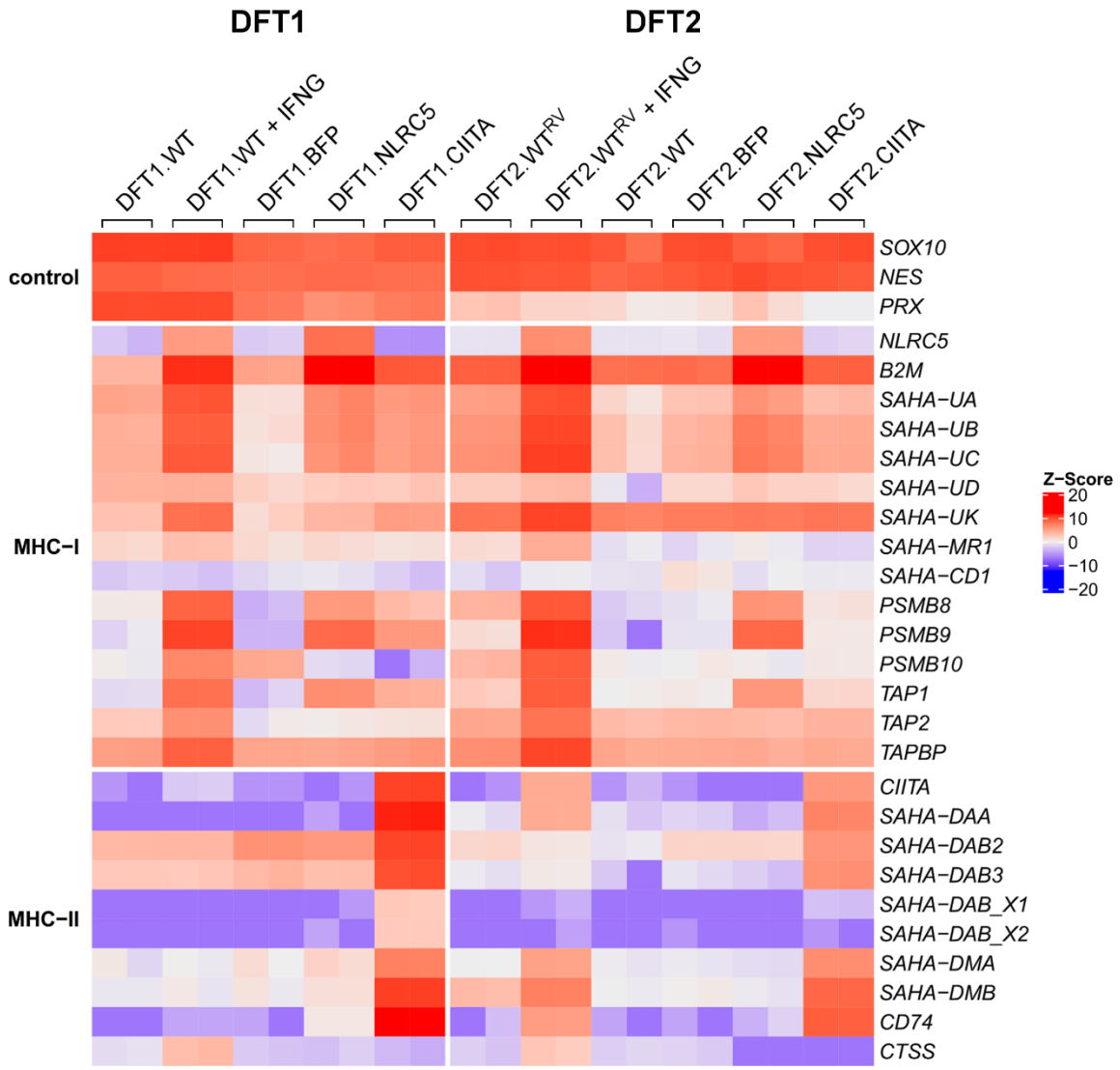

691

692 Figure 2. Heatmap showing relative expression of genes involved in MHC-I and MHC-II
693 antigen processing and presentation in wild type, IFNG-treated, BFP- (vector control),
694 NLRC5-, and CIITA-expressing DFT1 and DFT2 cells. Z-scores were calculated from
695 $\log_2$TPM expression values and scaled across each gene (rows). High and low relative
696 expression are represented by red and blue, respectively. Replicates per treatment (*N*=2) are
697 included in the heatmap.

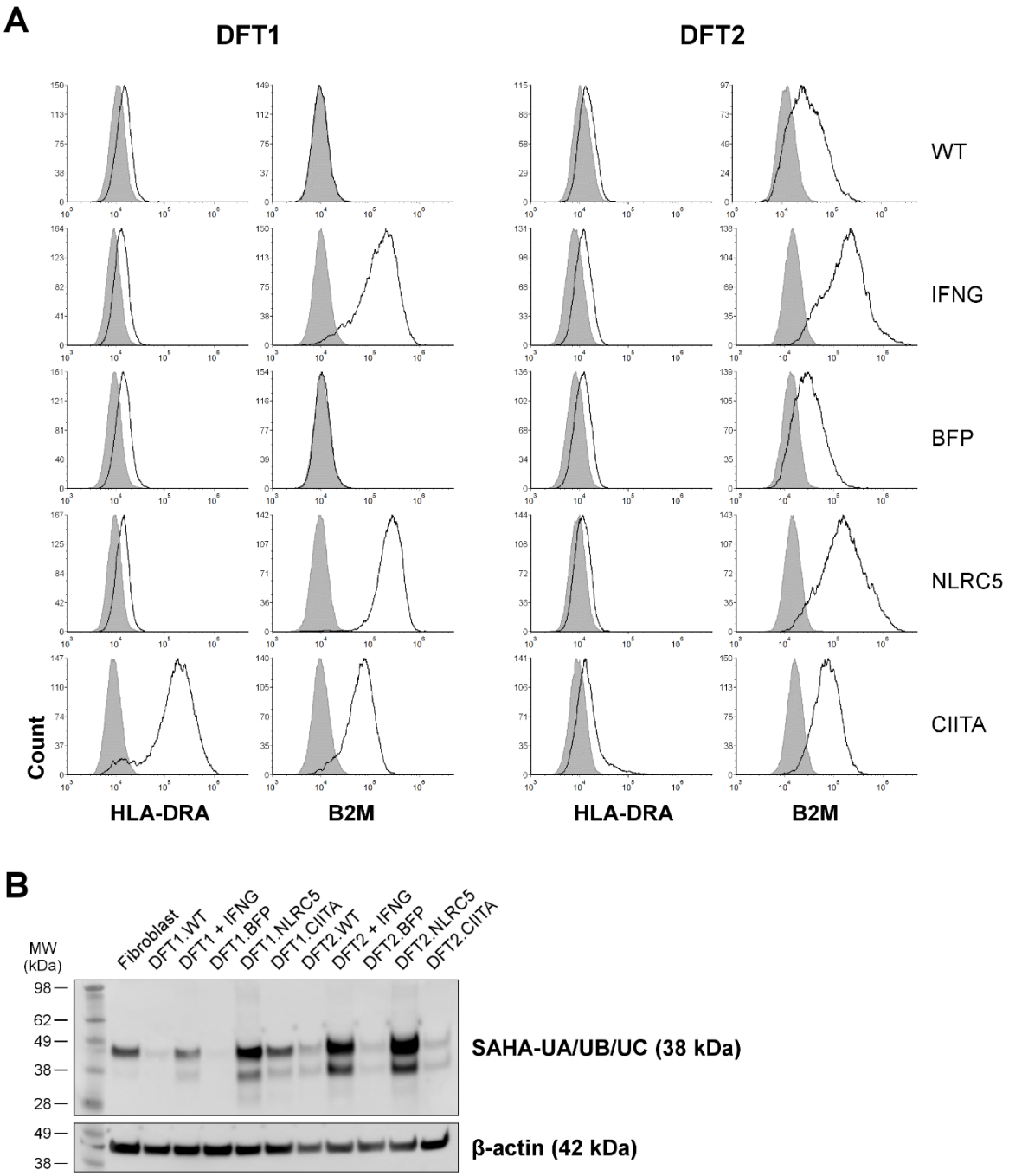

Figure 3. Expression of MHC-II, B2M and MHC-I in DFT1 and DFT2 cell lines. (**A**) Wild type (WT), IFNG-treated (IFNG), vector-only control (BFP), NLRC5-overexpressing (NLRC5) or CIITA-overexpressing (CIITA) DFT1 and DFT2 cells were analysed by flow cytometry for B2M and MHC-II expression using antibodies against surface devil B2M or intracellular HLA-DR alpha chain (HLA-DRA), respectively (*solid line*). B2M and MHC-II expressions were overlaid with a secondary antibody-only control (*shaded area*). The results shown are representative of *N*=3 replicates/treatment. (**B**) Cell lysate from devil fibroblast, DFT1 and DFT2 cell lines was incubated with an antibody against MHC-I heavy chain genes SAHA-UA/UB/UC for western blot analysis of MHC-I expression. β-actin was included as a loading control. *MW*, molecular weight.

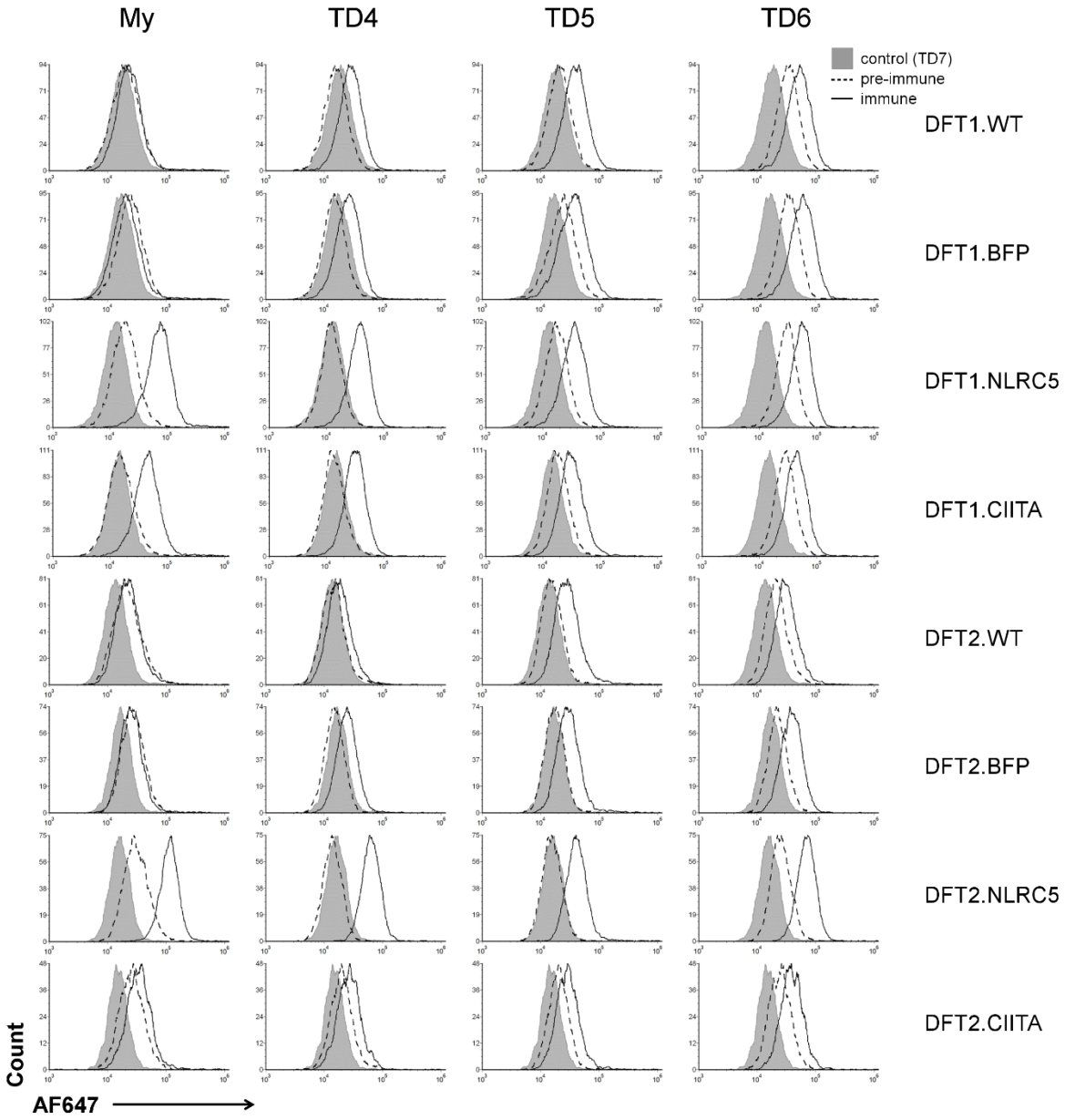

Figure 4. Flow cytometric analysis of serum antibody response towards DFT1 and DFT2 cells overexpressing CIITA. Sera from four devils (My, TD4, TD5, TD6) with antibody responses to MHC-I^{+} DFT1 cells after DFT1 infection (immune) were used. Antibody binding was compared against wild type (DFT.WT), vector-only (DFT.BFP) and NLRC5-overexpressing cells (DFT.NLRC5). Serum collected prior to infection (pre-immune) and from a non-infected devil (TD7) were included as negative controls. *AF647*, Alexa Fluor 647.